

## Strengthening Mechanisms in Al-Alloy/Carbon Black Nanocomposites

T. Prasad<sup>1</sup> and A. Chennakesava Reddy<sup>2</sup>

<sup>1</sup>*Research Scholar, Department of Mechanical Engineering,  
JNTUH University Hyderabad., India.*

<sup>2</sup>*Professor, Department of Mechanical Engineering,  
JNTUH University, Hyderabad, India.*

### Abstract

The aim of this research paper was to analyze the strengthening mechanisms in Al-Alloy/Carbon black nanocomposites. The matrix materials were AA6061, AA6063 and AA7020 aluminum alloys. The reinforcement was nickel-coated carbon black nanoparticles. Tensile tests were conducted to find strengths of the composites. Also, analytical models were employed to validate the experimental results. The important strengthening mechanisms in Al-alloy/CB nanocomposites were evolved in terms dimensionality (0-D, 1-D and 2-D). Indirect strengthening was more predominant instead of direct strengthening in Al-alloy/CB nanocomposites.

**Keywords:** AA6061, AA6063, AA7020, carbon black nanoparticles, strengthening mechanisms.

### 1. INTRODUCTION

It is very interesting to study the reinforcement mechanisms of the metal matrix composite (MMC) because it is the material for advanced technology, high temperature applications where high strength/stiffness to-weight ratio is required. Most of the studies on MMC have focused on aluminum (Al) as the matrix metal. The reinforcing particles with different physical characteristics in the aluminum matrix material give rise to mismatch at the interface. This condition is favorable to increase the strength as it increases the dislocation density and, is also effective in nucleating new grains. The reinforcing particles stabilize grain size by pinning of grain boundaries, which increases strain rate sensitivity and causes super plasticity at high strain rate (Iseki, et. al, 1984.,

Ishikawa, et. al, 1984., Arsenault, 1984). The main problem in aluminum matrix composites is the cavitation which limits the elongation. The grain boundary sliding due to the presence of reinforcing particles is increased by the extent of cavitation. The cavitation problem minimizes the use of very fine reinforcing particles (Warren and Anderson, 1984). Crack initiation and cracks developed thereon can be minimized by uniform distribution of reinforcing particles. During the precipitation dispersoids modify the microstructure. The increased dislocation density at the interface also enhances the kinetics of precipitation during ageing.

The elastic moduli of composites are higher compared to non-reinforced matrix at elevated temperatures (Tiwari, et. al., 1979). The volume fraction of reinforcement and interfacial strength are crucial for effective transfer of load from the matrix to the reinforcement and consequently in strengthening the composites. The volume fraction of interfacial strength and reinforcement is critical in order to efficiently move the load from the matrix to the reinforcement and thus to reinforce the composites. It is possible to optimize the wear and tear properties of the composites by using variety of reinforcements with different volume fractions. The ceramic reinforcements contribute to lower the coefficient of thermal expansion, increase hardness and stiffness and specific strength (Chen and Rigney, 1985., Gopinath, 1979).

Since testing of MMCs is both time consuming and expensive, computational studies are required to effectively characterize the microstructures and predict their characteristics – both plastic and elastic. Extensive analytical models were used to estimate the elastic properties of the particulate-reinforced metal matrix composites (Chawla and Shen, 2001).

The advance of innovative materials, which are lighter in weight, proceeds due to demands for more efficiency in applications such as aerospace, automobiles. The use of metals such as aluminum has increased in addressing this problem, but there is a need for lightweight materials that offer even superior mechanical and physical properties. One choice is to create composites combining a metal alloy with a second material which can further boost performance. Carbon black (CB) is a cheaply available as compared to graphite and other materials. Hence, the scope of present research work was on fabricating and testing of nickel-coated CB nanoparticles reinforced aluminum metal matrix composites.

## **2. MATERIALS AND METHODS**

### **2.1 Materials**

In the current work of research, the materials used for the matrix constituent were AA6061, AA6063 and AA7020. AA6061 is a precipitation hardening aluminum alloy. AA6063 possesses good mechanical properties and enables heat treatment. AA7020 is also heat treatable alloy. Carbon black is a material with high economic importance containing pure carbon which is produced through specific combustion processes. Highly structured carbon black provides higher viscosity, greater electrical conductivity and easier dispersion. Hence, in the present work, coated carbon black (CB)

nanoparticles were used as reinforcement. In the current study, carbon black nanoparticles were coated with nickel to avoid a reaction between carbon black and aluminum alloy. The average size of nickel pre-coated carbon black nanoparticles was 100 nano meter. The carbon black nanoparticles structure is spherical, as shown in Figure 1.

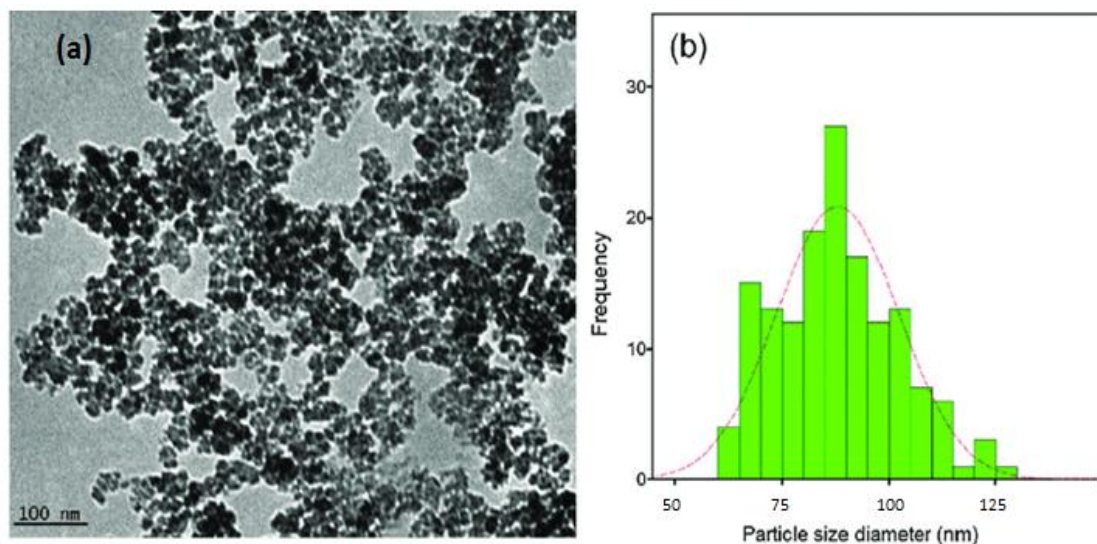


**Figure 1:** Morphology of CB nanoparticles.

## 2.2 Fabrication of carbon black-based MMCs

In the present research work, nickel-coated CB nanoparticles reinforced Al-MMCs were fabricated using two-step stir casting process. The carbon black reinforcement particulate volume fractions were 10, 20 and 30 percentages. The aluminum alloy matrix material is melted in resistance furnace using graphite crucible for carrying molten metal alloy. A flux which is a mixture of chloride and fluoride salts was used to reduce oxidation causing due to penetration of atmospheric hydrogen. Tetrachloroethane (in solid form) is used to degasification of molten alloy. The crucible was withdrawn from the furnace with molten metal and treated with sodium additive and its temperature is lowered only below the temperature of the liquids in order to melt semi-solid state. At this stage pre-heated (500<sup>0</sup>C for 1hour) nickel-coated CB nanoparticles were added to the semi-state liquid melt. Manually, the molten alloy with nickel coated CB nanoparticles was stirred thoroughly for 15 minutes. Following manual stirring, the semi-solid melt in the resistance furnace was reheated to a full liquid state followed by automatic mechanical stirring using a mixer to make the melt homogeneous at 200 rpm for around 10 min. A dip-type thermocouple was used to measure temperature of molten metal. The dross removed melt by the compressed organ gas of 3 bar was filled in the preheated cast iron die.(A.C.Reddy 2015).

## 2.3 Testing Practices of CB Nanoparticles Reinforced Al-MMCs

The as-cast composite samples were cut to test tensile strength, elastic modulus and for microstructural evaluation. Two samples were used for each test. A solution treatment at 500<sup>0</sup>C was applied for 1 hour just before composite samples were tested, followed by a quenching in cold water. The samples were then aged for 100 hours naturally at room temperature.

Flat rectangular specimens (Figure 2) are prepared from Heat-treated samples for tensile tests and they were placed in the grips of a 20 T capacity Universal Test Machine (UTM) at a specified grip separation, it was pulled until failure. The test speed was 2 mm / min (as with ASTM D3039). For determining elongation, a strain gauge was used as shown in Figure 3.

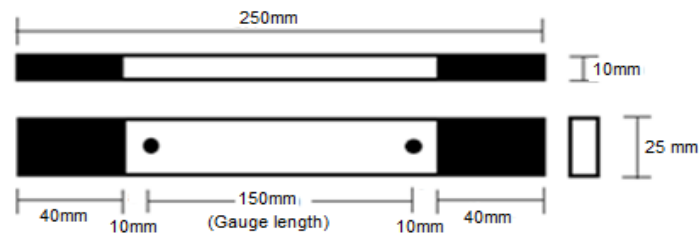


**Figure 2:** Shape and dimensions of tensile specimen.

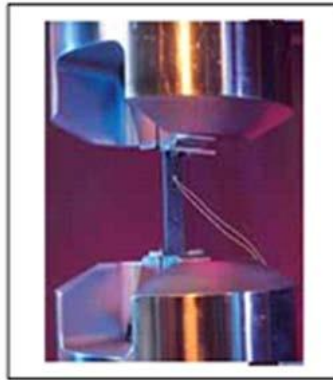


**Figure 3:** Tensile Test.

### 3. ANALYTICAL MODELS TO PREDICT STRENGTH AND MODULUS OF COMPOSITES

The strength and elastic modulus of Al alloy metal matrix composites depends on the strength and rigidity of the weakest field and metallurgical occurrences therein (AC Reddy, 2011a). Although numerous theories of composite strength and elastic modulus have been published, none is universally accepted. The present analytical study of nickel-coated CB nanoparticles reinforced Al-MMCs employed the determination of composite's strength and elastic modulus based on the analytical models established by AC Reddy (2011b) considering various volume fractions of CB nanoparticles. Comparison was made between the analytical results of composite's strength and elastic

modulus as obtained by using the analytical models by AC Reddy (2011b) respectively with the models of Pukanszky et. al (1988) and Ishai and Cohen (1967).

Considering adhesion, precipitate formation, particle size, agglomeration, voids / porosity, dislocation obstacles and the particle / matrix interfacial reaction, the formula as established by AC Reddy (2011a) for the Composite strength is shown:

$$\sigma_c = \left[ \sigma_m \left\{ \frac{1-(v_p+v_v)^{2/3}}{1-1.5(v_p+v_v)} \right\} \right] e^{m_p(v_p+v_v)} + k d_p^{-1/2} \quad (1)$$

$$\text{where, } k = \frac{E_m m_m}{E_p m_p} \quad (2)$$

$\sigma_c$  is the strength of composite;  $\sigma_m$  is the strength of matrix. The volume fractions of voids/porosity and nanoparticles in the composite are  $v_v$  and  $v_p$  respectively. The Poisson's ratios of the nanoparticles and matrix are  $m_p$  and  $m_m$  respectively;  $d_p$  is the mean nanoparticle size (diameter). The elastic module of the matrix and nanoparticle are  $E_m$  and  $E_p$  respectively. Young's modulus is a measure of a material's rigidity, and a quantity used to describe materials. It is known that for isotropic materials elastic modulus is same in all directions and it is a measure of stiffness of the material.

Analytical model established by Pukanszky et.al (1988) gives an empirical relationship between strength of composite ( $\sigma_c$ ) and strength of matrix ( $\sigma_m$ ) as mentioned below:

$$\sigma_c = \left[ \sigma_m \left( \frac{1-v_p}{1+2.5v_p} \right) \right] e^{Bv_p} \quad (3)$$

where, An empirical constant B is dependent on particle surface area, interfacial bonding strength, and particle density. The B value varies in between 3.49 to 3.87. The Pukanzky empirical relationship as given in Eq. (3) gives the ultimate strength of the particulate metal matrix composite which dependent on the strong particle-matrix interfacial bonding. While considering the Pukankzy's empirical relationship, necessary care has been taken about the Particulate involvement in composite and interfacial bonding between the nanoparticles / matrix, particle size, precipitate formation, agglomeration, voids / porosity and dislocation barriers.

While the present work was aimed at the development and characterization of CB nanoparticles reinforced Al-MMCs, a study on the determination of elastic modulus is very important to assess the deformability of these composites when subjected to different loads. Purna Irawan and Sukania, (2015) have stated that elastic modulus is an essential parameter in the analysis of composites. The normal property of elastic modulus is usually found from a conventional tensile testing. Ishai and Cohen (1967)

stated that, in many composites, anisotropy can be seen and accordingly they developed the following empirical relationship by considering unvarying stress applied and estimated ratio of composite elastic modulus ( $E_c$ ) and matrix ( $E_m$ ) as given below:

$$\frac{E_c}{E_m} = 1 + \left( \frac{1+(\delta-1)v_p^{2/3}}{1+(\delta-1)(v_p^{2/3}-v_p)} \right) \quad (4)$$

where,  $\delta = \frac{E_p}{E_m}$  (5)

The elastic module of composite, matrix and nanoparticles are  $E_c$ ,  $E_m$  and  $E_p$  respectively. Eq. (3.5) is an upper-bound equation and therefore particle and matrix are believed to be in a macroscopically homogenous state, and the interface adhesion is fine. Accordingly the lower-bound equation is given by

$$\frac{E_c}{E_m} = 1 + \left( \frac{v_p}{\delta/(\delta-1)-v_p^{1/3}} \right) \quad (6)$$

Considering the effect of voids/porosity and anisotropy in the composite, AC Reddy (2011b) has also established analytical model to find the elastic modulus of the composites as given below:

$$\frac{E_c}{E_m} = \left( \frac{1-v_v^{2/3}}{1-v_v^{2/3}+v_v} \right) + \left( \frac{1+(\delta-1)v_p^{2/3}}{1+(\delta-1)(v_p^{2/3}-v_p)} \right) \quad (7)$$

Also, estimation of elastic modulus (upper bound) by Rule of Mixtures (ROM) is given below:

$$E_c = E_m v_m + E_p v_p \quad (8)$$

The lower bound equation to find the elastic modulus by Rule of Mixtures is also given below:

$$E_c = \left( \frac{v_p}{E_p} + \frac{v_m}{E_m} \right)^{-1} \quad (9)$$

#### 4. RESULTS AND DISCUSSION

The increase in content of carbon black nanoparticles in the composite, the load transfer from the matrix to the nanoparticle increased as shown in figure 4. The load transfer from the matrix to CB nanoparticles in AA6061/10%CB, AA6063/10%CB and AA7020/10%CB is about 7MPa. The load transfer from the matrix to CB nanoparticles

in AA6061/20%CB, AA6063/20%CB and AA7020/20%CB is respectively, 14MPa, 12MPa and 17MPa. The load transfer from the matrix to CB nanoparticles in AA6061/30%CB, AA6063/30%CB and AA7020/30%CB is respectively, 41MPa, 34MPa and 45MPa.

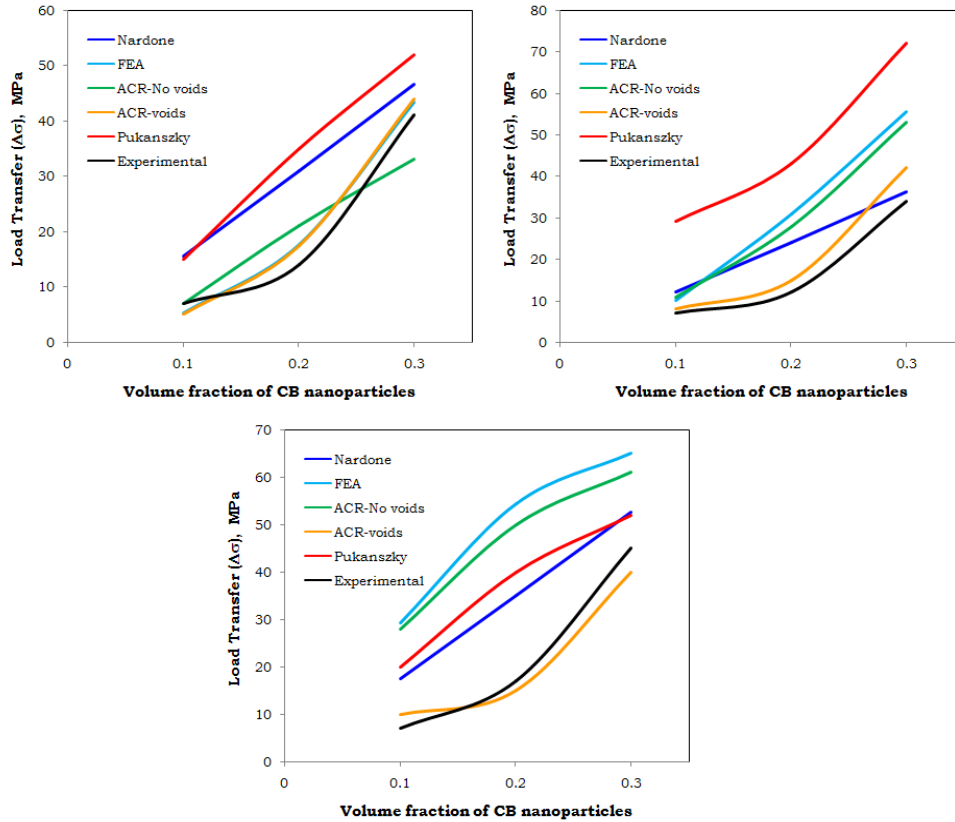


**Figure 4:** Load transfer from matrix to nanoparticles: (a) AA6061/CB, (b) AA6063/CB and AA7020/CB composites.

#### 4.1 Strengthening Mechanisms CB Nanoparticles Reinforced Al-MMCs

The mechanisms of strengthening identified in MMCs may be divided into two groups, direct and indirect strengthening. Throughout the direct strengthening of particulate-reinforced MMCs, the load is moved from the weaker matrix, via the matrix / reinforcement interface, to the usually higher stiffness reinforcement. Due to the lower aspect ratio of particulate materials (spherical shape CB nanoparticles), load transfer is not efficient in the particulate reinforced MMCs (Chawla et. al, 2000). Arsenault and Shi (1986) have stated that the strengthening mechanism in as-cast MMCs is indirect strengthening mechanism. Hence, indirect strengthening mechanism may play predominant role in the nickel-coated CB nanoparticles reinforced Al-MMCs. The Punching results of thermally-induced dislocation in indirect strengthening of the matrix. As Al alloy/CB MMCs were prepared in the present work via stir casting route wherein a high stiffness CB nanoparticles were reinforced in AA6061, AA6063 and

AA7020 matrix Al-alloys, Usually thermal mismatch between the high Alloy matrix and the low CB nanoparticles is very large. The linear thermal expansion coefficient of AA6061, AA6063 and AA7020 Al-alloys are, respectively  $23.2 \times 10^{-5} \text{ K}^{-1}$ ,  $23.5 \times 10^{-6} \text{ K}^{-1}$  and  $23.1 \times 10^{-6} \text{ K}^{-1}$ . The linear thermal expansion coefficient of carbon black is  $4.5 \times 10^{-6} \text{ K}^{-1}$ . The thermal mismatch between the said Al-alloys and carbon black is about  $19.0 \times 10^{-6} \text{ K}^{-1}$ . Thus dislocations form at the reinforcement / matrix interface after solidification due to high thermal inconsistencies. AA6061, AA6063 and AA7020 alloys are age-hardenable alloys. In age-hard matrix Al alloys, the thermally induced dislocations serve as heterogeneous nucleation sites during aging treatment for precipitate formation (as in the present research work T6 heat treatment). In the present work, the tensile strength was increased with increased content of CB nanoparticles in the matrix Al alloys (AA6061, AA6063 and AA7020). The increase in the fraction of the reinforcement volume increases the amount of indirect strengthening, since there is a larger amount of interfacial space for punching dislocation to occur. Krajewski et. al (1993) have stated that the precise amount of indirect strengthening is more difficult to calculate than the direct strengthening contribution. Hence, empirical or analytical models were used to find strengthening effect in the MMCs. The same was followed in the present work to acquire knowledge about the strengthening mechanism and to validate the experimental results. In the present research work, Pukanszky et. al (1988) model, AC Reddy models without voids/porosity (2011a) and with voids/porosity (2011b) were used to find the strength of MMCs and Ishai and Cohen (1967) model and AC Reddy (2011b) model were used to find elastic modulus of MMCs. The results obtained from these models were compared with experimental results and reasons for the deviation were also discussed. The background strengthening mechanisms involved in the said models are discussed in the following paragraphs for detailed understanding.

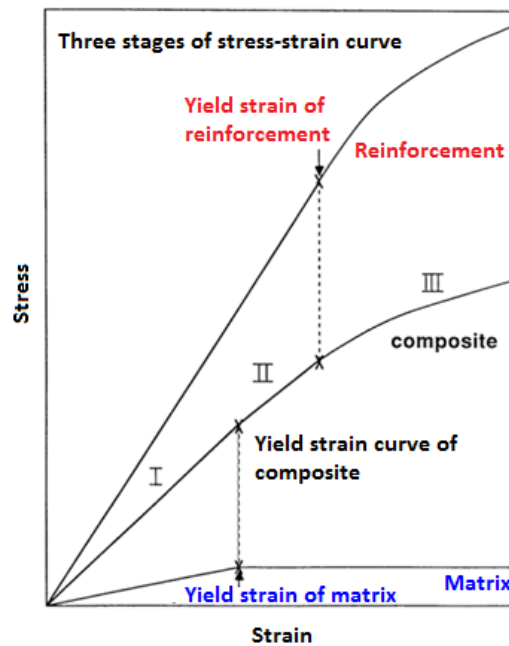


**Figure 5:** Stress-strain curves of MMCs.

The required mechanical properties of Al-MMCs are yield strength, ultimate tensile strength, work-hardening rate, stiffness (elastic modulus) and fracture toughness. As shown in figure 5 the stress-strain curves for MMCs represent three stages. In Stage I, both matrix and reinforcement remain elastic; in Stage II – matrix deforms plastically and reinforcement remains elastic; and in Stage III – both matrix and reinforcement deform plastically. At a relatively low stress, microplasticity exists in MMCs, which leads to a small deviation from linearity in the stress-strain curve. Microplasticity in the MMCs was due to stress concentrations in the matrix at the reinforcing poles (Chawla et. al, 1998). The incorporation of particles in the matrix results in an increase in work hardening in the MMCs. The higher work-hardening rate observed in Al-MMCs reinforced by CB nanoparticles is thus due to geometric constraints imposed by the existence of CB nanoparticles. As the volume fraction of CB nanoparticles increased, more load was transferred to the reinforcement, which also results in a higher ultimate tensile strength.

#### 4.1.1 Zero-D strengthening mechanism

The classification of strengthening mechanisms in the MMCs is based on their dimensionality such as 0-D, 1-D and 2-D (Courtney, 1990). At 0-D, precipitate and solid solution stabilize with structure supporting particulates. Solid solution strengthening is a method of improving metal strength by adding solute atoms from another element to inhibit movement through dislocations in the metal's crystal lattice. The heat treatment method used to improve the yield strength of aluminum alloys is precipitation hardening, also called particle hardening. The heat treatment method used to improve the yield strength of aluminum alloys is precipitation hardening, also called particle hardening. Precipitation hardening imparts changes in solid solubility with temperature to create small particles of an impurity phase that hinder dislocation movement, or defects in the lattice of a crystal. Since the dislocation is often the dominant carrier of plasticity, this helps to harden the material.

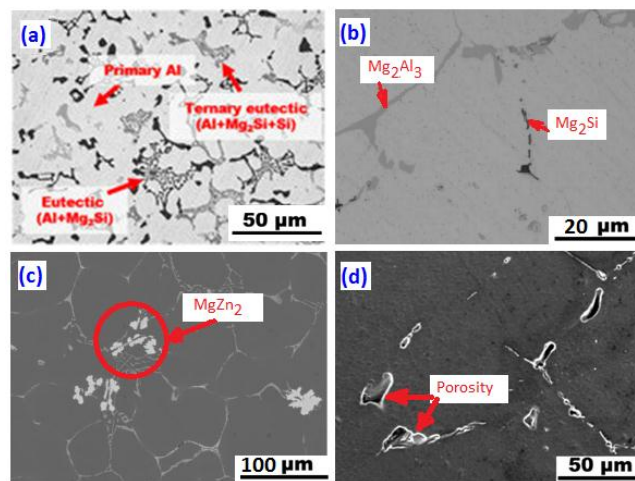


**Figure 6:** Precipitated compounds and porosity: (AA6061 alloy, (b) AA6063 alloy and (c) AA7020 alloy.

AA6061 Alloy is an aluminum alloy hardening precipitation which contains magnesium and silicon as its major alloy elements. Similarly AA6063 has magnesium and silicon as the alloying elements. AA7020 alloy has zinc added as the main alloying element. In the present research work, T6 precipitation hardening heat treatment was given to CB nanoparticles reinforced Al-MMCs. The ultimate tensile strengths of T6 heat treated AA6061, AA6063 and AA7020 aluminum alloys are 310 MPa, 241 MPa and 350 MPa respectively. On account of T6 heat treatment, the main precipitate in AA6061 matrix alloy is  $Mg_2Si$  (figure 6a) compounds. The main precipitates in AA6063 matrix alloy are  $Mg_2Si$  and  $Mg_2Al_3$  (figure 6b) compounds. The main precipitate in AA7020 matrix alloy is  $MgZn_2$  (figure 6c) compounds (Andersen et. al, 2018; Fine, 1975). Due to T6 Heat treatment grain boundary sizes often change, but the effect on strength is not as significant as the precipitation. Porosity is also present in the matrix regions (figure 6d). Porosity diminishes the strength of composites.

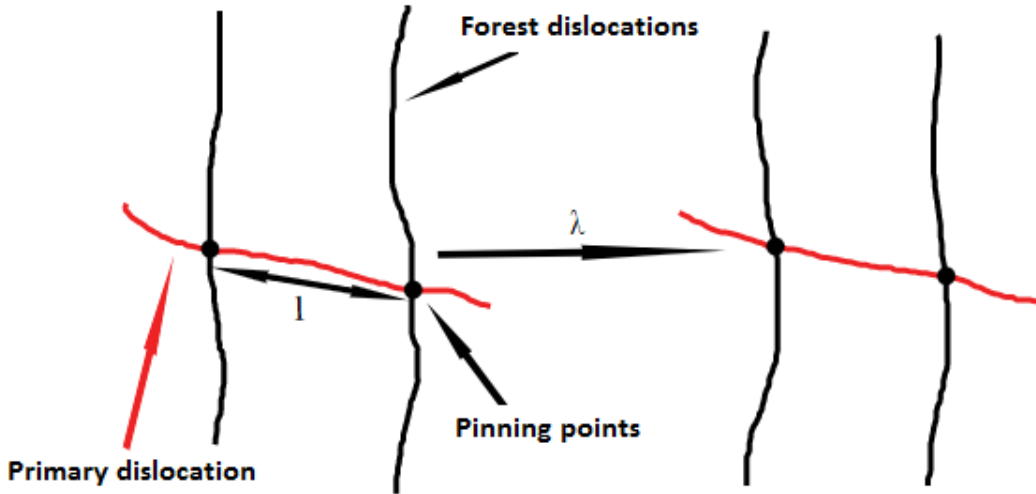


Figure 7: Forest hardening.

#### 4.1.2 One-D strengthening mechanism

At 1-D, forest hardening occurs with line dislocations as the mechanism for hardening. In the forest hardening, as they collide with the forest dislocations, the active dislocations that glide in the primary slip plane get stuck at obstacles as shown in figure 7. This kind of mechanism is largely observed in the CB nanoparticles reinforced Al-MMCs. Ebeling and Ashby (1966) have showed that most of the experimental data at a few percent to large plastic strains obey the following shear stress/shear strain relation:

$$\tau = \tau_y + \beta G \sqrt{\frac{bc_i \gamma}{d}} \quad (10)$$

where,  $\tau$  and  $\gamma$  are the applied shear stress and plastic strain, respectively,  $b$  and  $G$  are the Burgers vector and shear modulus of the matrix material  $c_i$  and  $d$  are the volume

fraction and mean diameter of nanoparticles, respectively and  $\beta$  is a dimensionless constant equal to  $0.24 \pm 0.04$ . Work hardening stress  $\tau - \tau_y$  is proportional to  $\sqrt{\gamma}$ . Ashby has attempted to explain this square root dependence on shear strain by proposing the relaxation mechanism of the large misfit strain at the matrix-particle interface, which increases with increasing plastic shear strain.

In the present research work, CB nanoparticle reinforced in the matrix Al alloy is subjected to compressive stress which results in a homogeneous shear strain  $\gamma$  in the  $x$ -direction (loading direction) as shown in figure 8. Then an initially spherical nanoparticle deforms to an ellipsoid with longer axis along the loading direction. If the CB nanoparticle is removed from the ellipsoidal hole from the matrix, while keeping the compressive stress, then the shape of the ellipsoidal hole would become more elongated, shown as solid line in figure 8(b) along the loading direction, the  $x_1$ -axis. In order to bring back to the ellipsoidal shape in a loaded dispersion-hardened alloy before the removal of the nanoparticle, one must apply a set of displacements,  $u_1$  along the  $x_1$ -axis and  $u_2$  along the  $y_1$ -axis, figure 8(b). This set of displacement field is equivalent to punching out  $n$  dislocations loops with Burgers vector  $b$  along four directions. The displacements  $u_1$ ,  $u_2$  at the matrix-particle interface take the following maximum values:

$$(u_1)_{max} = \frac{\gamma d}{4} \text{ and } (u_2)_{max} = -\frac{\gamma d}{4} \quad (11)$$

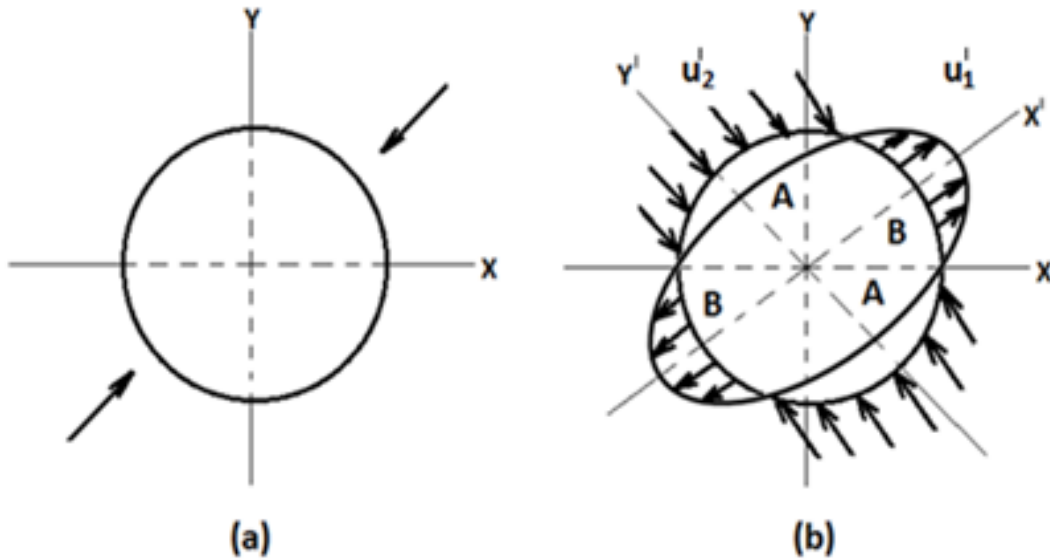


**Figure 8:** Ashby model: (a) CB particle reinforced in matrix Al alloy subjected to compressive stress and (b) displacements  $u_1$ ,  $u_2$  applied to ellipsoid to bring back to its original spherical shape.

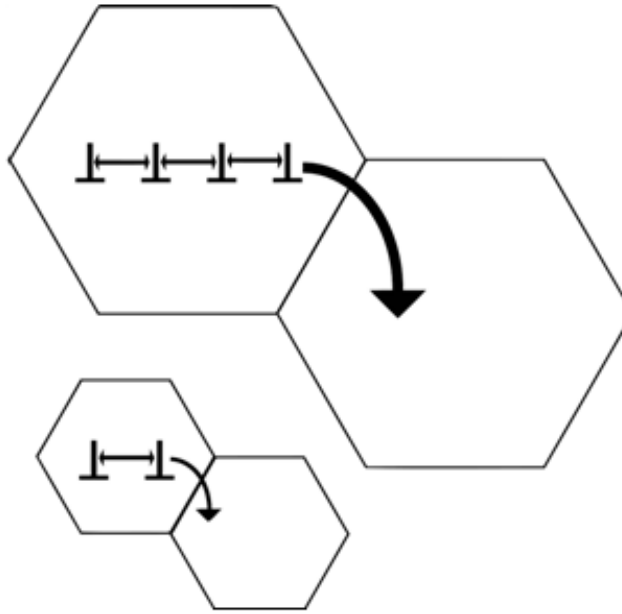


**Figure 9:** Grain boundary mechanism.

#### 4.1.3 Two-D strengthening mechanism

At 2-D, the grain boundary is strengthened with surface energy of granular interfaces providing an increase in strength. In the strengthening of grain boundaries, the grain boundaries act as pinning points which impede further spread of dislocation. Since the lattice structure of the neighboring grains varies in orientation, to change directions and transfer into the neighboring grain requires more energy for a dislocation. Since grains typically have varying crystallographic orientations, the boundaries of grain appear. Slip motion may occur while undergoing deformation. Boundaries of grain serve as an impediment to dislocation for the following two reasons (William Jr., 1985):

1. The dislocation must change its direction of motion due to the different orientation of the grains.
2. Discontinuity of gliding planes from grain one to grain two.

The stress needed for moving a dislocation from one grain to another to plastically deform a substance depends on the size of the grain. The composite material with a larger grain size is capable of making more dislocations pile up, resulting in a stronger driving force for dislocations to transfer from one grain to another. (Lesuer and Sherby, 2007). This needs less force to transfer a dislocation from a larger grain than from a smaller grain, resulting in higher yield stress composite materials with smaller grains as shown in figure 9.

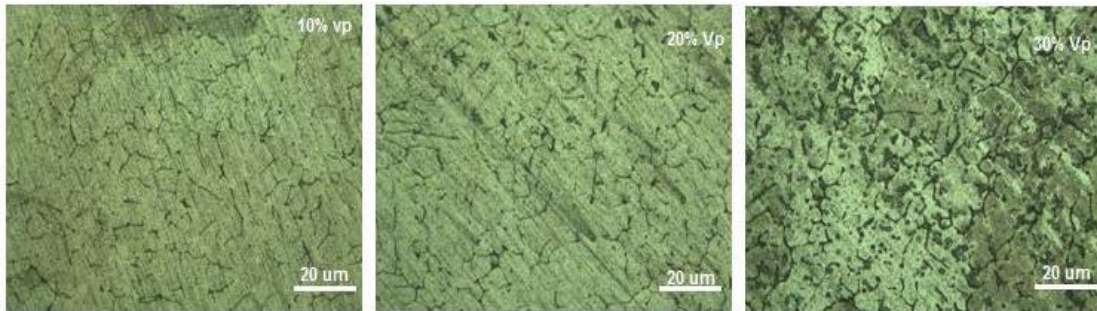


**Figure 10:** Optical microstructures of AA6061/carbon black nanocomposites.

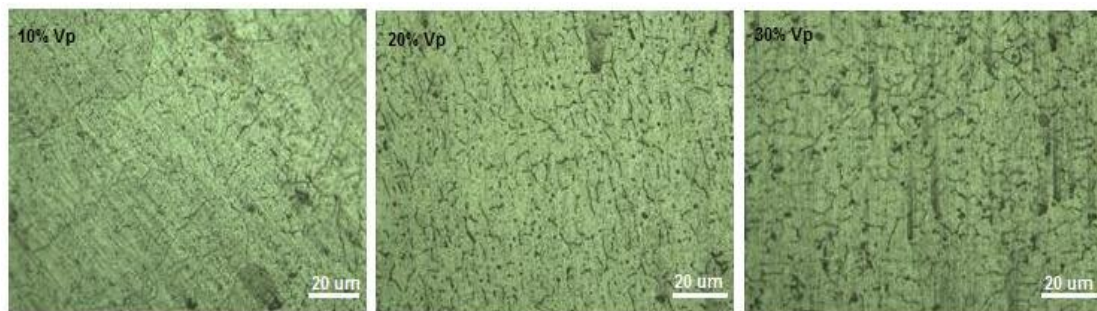


**Figure 11:** Optical microstructures of AA6063/carbon black nanocomposites.

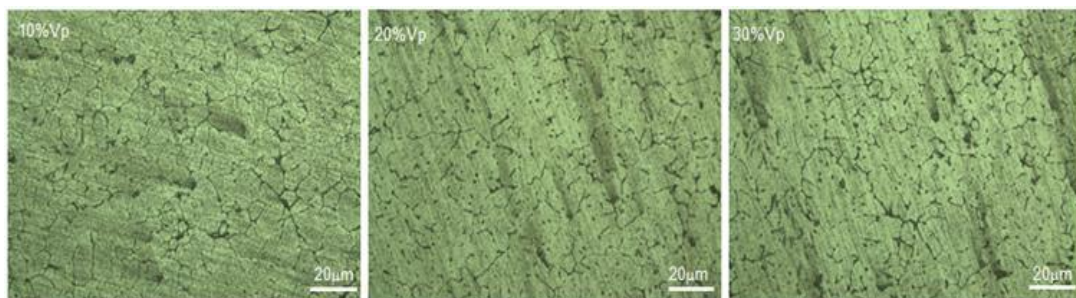


**Figure 12:** Optical microstructures of AA7020/carbon black nanocomposites.

### 3.1.4 Dispersion strengthening mechanism

Dispersion hardening involves the inclusion of small, hard particles (as in the present work, CB nanoparticles) in the matrix alloy, thus restricting the movement of dislocations, and thereby raising the strength properties (Soboyejo, 2003). Figure 10, Figure 11 and Figure 12 reveals the optical microstructures of AA6061, AA6063 and AA7020 nanocomposites respectively. In the said three figures, it is identified that the CB nanoparticles are randomly dispersed in the AA6061/ AA6063/AA7020 matrix alloys. The densities of AA6061, AA6063 and AA7020 alloys and nickel-coated CB nanoparticles are respectively, 2.7 g/cc, 2.71 g/cc, 2.78 g/cc and 2.56 g/cc. The difference in densities of matrix and reinforcement are nearly equal which gives rise to

random distribution of nickel-coated CB nanoparticles in the matrix alloy. Figure 13 illustrates why dislocations can interact with the reinforced particule. The dislocation will curve around the hard reinforced particle, forming a dislocation loop as it passes over the particle.

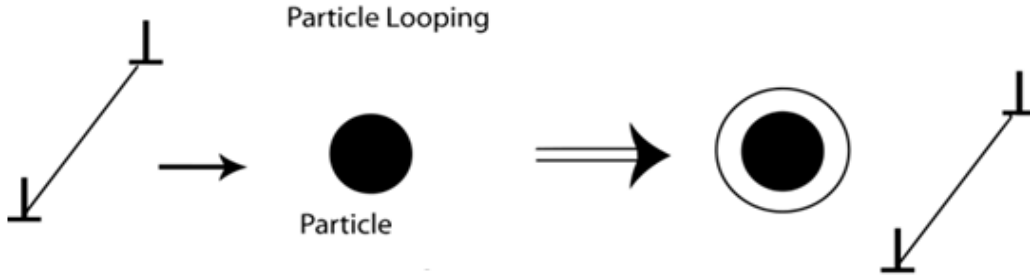


**Figure 13:** Dispersion strengthening mechanism.

### 3.1.5 Load transferring mechanism

The transition of load from the soft matrix Al alloy to rigid and hard CB nanoparticles under the applied external load leads to the strengthening of the matrix Al alloy. (AC Reddy, 2011c). The load transfer increases with increasing content in the Al matrix alloys. An updated model of the Shear Lag proposed by Nardone and Prewo (1986) is widely used to estimate the contribution to reinforcing due to transfer of load in particulate-reinforced composites.

$$\Delta\sigma = v_p \sigma_m \left[ \frac{(l+t)A}{4l} \right] \quad (12)$$

Where  $v_p$  is the volume fraction of nano particles,  $\sigma_m$  is the unreinforced yield strength matrix,  $l$  and  $t$  are the particulate size parallel and perpendicular to the loading direction, respectively. For equiaxed particles case Eq.(4.3) reduces to

$$\Delta\sigma = \frac{1}{2} v_p \sigma_m \quad (13)$$

In all the composites, the values of lead transfer are approximately equal in AC Reddy (2011b) model with voids/porosity and experimental procedure. In the case of AA6061/CB composites, the values of lead transfer obtained from Nardone and Prewo (1986) model and Pukanszky et. al (1988) model are higher than the above-said models/methods. In the case of AA6063/CB composites, the values of lead transfer obtained from Pukanszky et. al (1988) model are higher than the all other models/methods; while the values of lead transfer obtained from Nardone and Prewo (1986) model lower than the all other models/methods. In the case of AA7020/CB

composites, the values of load transfer obtained from Nardone and Prewo (1986) model and Pukanszky et. al (1988) model are intermediate to the models/methods of without voids/porosity and with voids/porosity. Nardone and Prewo (1986) and Pukanszky et. al (1988) models are empirical models. The most matching analytical model is AC Reddy (2011b) model to the experimental values. The trend of load transfer is matching with Nardone and Prewo (1986) and Pukanszky et. al (1988) models.

### 3.2 Fracture Analysis

The SEM (scanning electron microscope) images of the fractured sections of tensile specimens are shown in figures 14, 15 and 16. In all the composites having 10% CB nanoparticles, the mixed mode i.e., ductile and brittle fracture is observed. As the volume fraction of CB nanoparticles increased to 20% and 30%, brittle fracture is noticed. This is due to agglomeration of CB nanoparticles at these volume fractions 20% and 30% of CB nanoparticles. The fracture of CB nanoparticles is not revealed in all the composites.

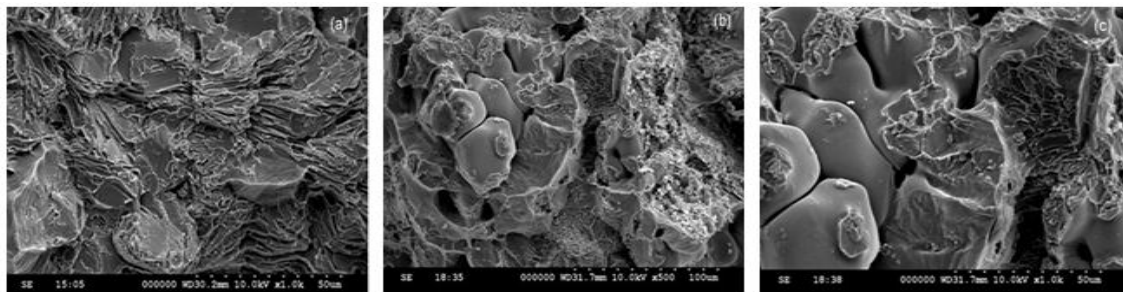


**Figure 14:** Fractographs of AA6061/CB composites: (a) 10%CB, (b) 20%CB and (c) 30% CB.

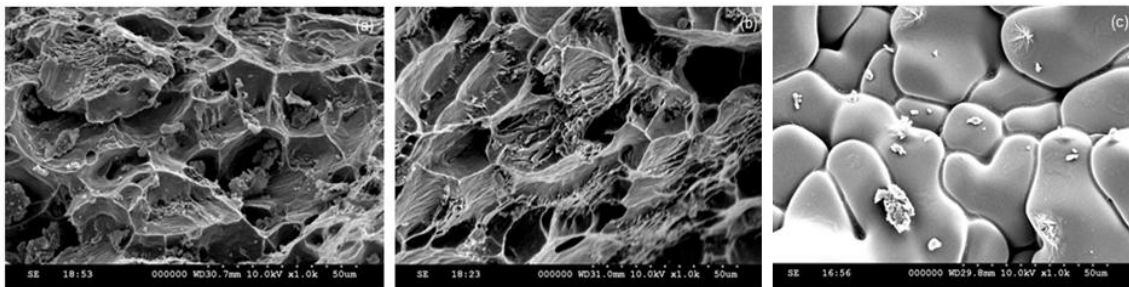


**Figure 15.** Factographs of AA6063/CB composites (a) 10% CB (b) 20% CB and (c) 30% CB

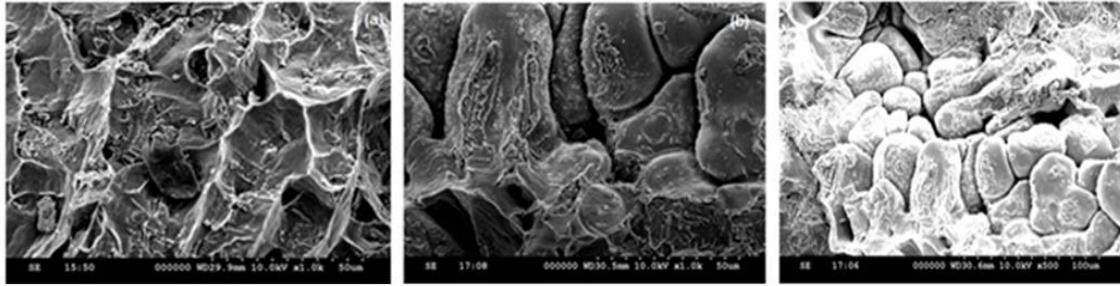


**Figure 16:** Factographs of AA7020/ CB composites (a) 10% CB (b) 20% CB and (c) 30% CB

## 5. CONCLUSIONS

The increase of CB content in AA6061/CB, AA6063/CB and AA7020/CB MMCs increases the tensile strength and elastic modulus and also increases the load transfer from the matrix to the nanoparticle. The load transfer from the matrix to CB nanoparticles in AA6061/10%CB, AA6063/10%CB and AA7020/10%CB is about 7MPa. The load transfer from the matrix to CB nanoparticles in AA6061/20%CB, AA6063/20%CB and AA7020/20%CB is respectively, 14MPa, 12MPa and 17MPa. The load transfer from the matrix to CB nanoparticles in AA6061/30%CB, AA6063/30%CB and AA7020/30%CB is respectively, 41MPa, 34MPa and 45MPa. Because of T6 heat treatment, the precipitate in AA6061 and AA7020 matrix alloys were, respectively  $Mg_2Si$  and  $MgZn_2$ . The precipitates in AA6063 matrix alloy were  $Mg_2Si$  and  $Mg_2Al_3$ . During plastic deformation CB nanoparticles reinforced Al-MMCs, the dislocation density increased due to thermal mismatch of about  $19.0 \times 10^{-6} K^{-1}$  between Al-alloys (used in this research) and CB nanoparticles. As a result, the number of such events continuously increased, thus leading to strain hardening through a mechanism called forest hardening. Another strengthening mechanism involved in CB nanoparticles reinforced Al-MMCs was grain boundary strengthening. The carbon black nanoparticles were randomly distributed in the AA6061/ AA6063/AA7020 matrix alloys. The load transfer increased with increasing content in the Al matrix alloys. The brittle fracture was revealed in the CB nanoparticles reinforced Al-MMCs.

## REFERENCES

- [1] Andersen, S.J., Marioara, C.D., Jesper, F., Wenner, S. and Holmestad, R., (2018), Precipitates in aluminium alloys, *Advances in Physics: X*, vol. 3(1), pp. 791-814.
- [2] Arsenault, R., (1984), The strengthening of aluminium alloy 6061 by fiber and platelet silicon carbide, *Material Science Engineering*, vol. 64(2), pp. 171-181.

- [3] Arsenault, R.J. and Shi, N., (1986), Dislocation generation due to differences between the coefficients of thermal expansion, *Materials Science and Engineering*, vol. 81, pp. 175-187.
- [4] Chawla, N., Jones, J.W., Andres, C. and Allison, J.E., (1998), Effect of SiC volume fraction and particle size on the fatigue resistance of a 2080 Al/SiC p composite. *Metallurgical and Materials Transactions A*, vol. 29, pp. 2843–2854.
- [5] Chawla, N., Habel, U., Shen, Y. L., Andres, C., Jones, J. W. and Allison, J. E., (2000), The effect of matrix microstructure on the tensile and fatigue behavior of SiC particle-reinforced 2080 Al matrix composites, *Metallurgical and Materials Transactions A*, vol. 31, pp. 531–540.
- [6] Chawla, N. and Shen, Y. L., (2001), Mechanical behavior of particle reinforced metal matrix composites, *Advanced Engineering Materials*, vol. 3(6), pp. 357-370.
- [7] Chen, L. H. and Rigney, D. A., (1985), Transfer during unlubricated sliding wear of selected metal systems, *Wear*, vol. 105(1), pp. 47–61.
- [8] Courtney, T. H., (1990), *Mechanical Behavior of Materials* (2nd ed.). Long Grove, IL: Waveland Press Inc.
- [9] Ebeling, R. and Ashby, M. F., (1966), Dispersion hardening of copper single crystals, *Philosophical Magazine*, 13 (124), pp. 805-834.
- [10] Gopinath, (1979), *Proceedings of National conference on aluminium metallurgy*, Iisc Bangalore, India, pp.289-294.
- [11] Iseki, T., Kameda, T. and Maruyama, T., (1984), Interfacial reactions between SiC and aluminium during joining, *Journal of Material Science*, vol. 19(5), pp. 1692-1698.
- [12] Ishai, O. and Cohen, I.J., (1967), Elastic properties of filled and porous epoxy composites, *International Journal of Mechanical Sciences*, vol. 9, pp. 539-546.
- [13] Ishikawa, T., Tanaka, J., Teranishi, H., Okamura, T. and Hayase, T., (1984), Process for the surface treatment of inorganic fibers for reinforcing titanium or nickel and product, U.S. Patent No. 4, 440, 571.
- [14] Krajewski, P.E., Allison, J.E. and Jones, J.W., (1993), The influence of matrix microstructure and particle reinforcement on the creep behavior of 2219 aluminum, *Metallurgical and Materials Transactions A*, vol. 24, pp. 2731–2741.
- [15] Lesuer, D.R; Syn, C.K; Sherby, O.D., (2007), Nano-subgrain strengthening in ball-milled iron, *Materials Science and Engineering: A*, vol. 463(1–2), pp.54–60.
- [16] Nardone, V.C., Prewo, K.M., (1986), On the strength of discontinuous silicon carbide reinforced aluminum composites, *Scripta Metalilurgica*, Vol. 20, pp. 43–48.

- [17] Pukanszky, B., Turscanyi, B. and Tudos, F. (1988), Effect of interfacial interaction on the tensile yield stress of polymer composites, *Elesvier*, pp.467-477.
- [18] Purna Irawan, A., Sukania, I. W., (2015), Tensile strength of banana fiber reinforced epoxy composites materials, *Applied mechanics and materials*, vol.776, pp.260-263.
- [19] Reddy, A. C., (2011a), Tensile fracture behaviour of 7072/SiCp metal matrix composites fabricated by gravity die casting process, *Materials Technology: Advanced Performance Materials*, vol. 26(5), pp. 257-262.
- [20] Reddy, A. C., (2011b), Evaluation of mechanical behaviour of Al-alloy/Sic metal matrix composites with respect to their constituents using Taguchi techniques, *i-manager's Journal of Mechanical Engineering*, vol. 1(2), pp. 31-41.
- [21] Reddy, A. C., (2011c), Strengthening mechanisms and fracture behavior of 7072Al/Al<sub>2</sub>O<sub>3</sub> metal matrix composites, *International Journal of Engineering Science and Technology*, vol. 3(7), pp. 6090-6100.
- [22] Reddy, A. C., (2015). Influence of Particle Size, Precipitates, Particle Cracking, Porosity and Clustering of Particles on Tensile Strength of 6061/SiCp Metal Matrix Composites and Validation Using FEA, *International Journal of Materials Science and Engineering*, vol. 42, pp. 1176-1186.
- [23] Soboyejo, W. O., (2003), Dispersion Strengthening, Mechanical Properties of Engineered Materials, Marcel Dekker, ISBN 0-203-91039-7.
- [24] Tiwari, S.N., Pathak, J.P. and Malhotra, S.L., (1979), Production of high leaded Al by impeller mixing, *Metals technology*, vol. 6, pp. 442-445.
- [25] Warren, R. and Anderson, C., (1984), Silicon carbide fibers and their potential for use in composite materials, Part II, *Composites*, vol. 15(2), pp. 101-111.
- [26] William Jr, C., (1985), *Materials Science and Engineering, An Introduction*, John Wiley & Sons, NY, NY.